Research Square

Preprints are preliminary reports that have not undergone peer review.
They should not be considered conclusive, used to inform clinical practice,
or referenced by the media as validated information.

Comparison of Deep Learning Reconstructed HASTE Sequence and Conventional BLADE Sequence for Liver T2-weighted Imaging

San-Yuan Dong
Zhongshan Hospital
Jia-Hui Wang
University Hospital of Bern
De-Zhen Guo
Zhongshan Hospital
Caixia Fu
Siemens Healthineers (Germany)
Dominik Nickel
Siemens Healthineers (Germany)
Wen-Tao Wang
Zhongshan Hospital
Xiao-Shan Chen
Zhongshan Hospital
Dan-Lan Lian
Zhongshan Hospital
Wei Sun
Zhongshan Hospital
Cai-Zhong Chen
Zhongshan Hospital
Meng-Su Zeng
Zhongshan Hospital
Ying Ding
Zhongshan Hospital
Sheng-Xiang Rao
raoxray@163.com
Zhongshan Hospital

Research Article

Keywords: Magnetic resonance imaging, T2-weighted imaging, Deep learning reconstruction, Liver Neoplasms, Image quality

Posted Date: November 1st, 2026

DOI: https://doi.org/10.21203/rs.3.rs-11068134/v1

License: This work is licensed under a Creative Commons Attribution 4.0 International License. Read Full License

Additional Declarations: No competing interests reported.

Abstract

Objectives

To compare the acquisition time, image quality, and T2WI signal characteristics of the T2-weighted deep learning (DL) reconstructed HASTE sequence with conventional T2-weighted BLADE sequence for liver MRI.

Methods

From July 2023 to March 2024, 309 patients with suspected liver lesions were prospectively included. The Mann-Whitney U test and paired Wilcoxon signed-rank test were used to assess qualitative and quantitative parameters. Intra-class correlation coefficient (ICC) and kappa coefficients were used to assess agreement between the two readers.

Results

The median acquisition time of the T2-weighted DL HASTE sequence was shorter than that of the BLADE sequence (34 seconds [IQR, 34–34 seconds] vs 169 seconds [IQR, 158–181 seconds], respectively; $P < 0.001$). Artifacts ($P < 0.001$), pancreatic duct margin ($P < 0.001$), homogeneity of fat suppression ($P = 0.002$), strength of fat suppression ($P < 0.001$), and conspicuity of the liver smallest lesion ($P < 0.001$) were significantly better for the T2-weighted DL HASTE sequence. Contrast-to-noise ratio (CNR) of liver lesions was significantly higher for the DL HASTE sequence ($P < 0.001$), especially for cysts ($P < 0.001$). The two sequences showed similar performance in the T2WI signal characteristics of focal liver lesions.

Conclusions

The T2-weighted DL HASTE sequence led to shorter examination time and higher image quality with comparable T2WI signal characteristics of focal liver lesions compared with the BLADE sequence.

Introduction

Magnetic resonance imaging (MRI) is one of the most important imaging modalities for evaluating the liver. In clinical liver MRI, T2-weighted imaging (T2WI) is critically important for the detection and characterization of liver lesions[1–4]. But it has been plagued by long scanning times and motion artifacts for a long time.

Modified multi-shot turbo spin echo (TSE) T2-weighted sequences based on radial scan techniques including BLADE (Siemens Healthcare, Erlangen, Germany) have been developed to reduce motion artifacts, but may prolong acquisition time[5, 6]. To ensure image quality, respiratory triggering or multiple breath-holds (≥ 4) are required for complete whole-liver imaging. Inconsistencies in liver positioning during each respiratory cycle or breath-hold can disrupt image continuity, thereby affecting overall image quality and the ability to observe lesions.

The half-Fourier acquisition single-shot TSE (HASTE) sequence is faster and more resistant to motion artifacts[7, 8], but results in decreased lesion/liver contrast-to-noise ratio (CNR) due to T2 decay during data acquisition and the weak intensity of the late echo signals[8]. Recently developed reconstruction algorithms with trainable components, referred to as deep learning (DL) reconstruction, promise higher acceleration factors while simultaneously increasing imaging quality[9, 10]. This DL reconstruction algorithm has also been successfully combined with HASTE sequence for single-breath-hold abdominal imaging[11–13].

Previous retrospective studies comparing the T2-weighted DL HASTE sequence on liver MRI with the BLADE sequence[12, 14, 15] and the conventional TSE sequence[16, 17] found that the DL HASTE sequence could reduce the acquisition time while improving image quality. Two prospective studies comparing the T2-weighted DL HASTE sequence on liver MRI at 3 T with the BLADE sequence[18] and the TSE sequence[19] reached similar conclusions. However, most of these studies focused on perceived image quality rather than on the T2WI signal characteristics of focal liver lesions, and their impact on lesion characterization has yet to be fully explored, especially in prospective studies. Additionally, previous studies had relatively small patient populations and a limited range of lesion types.

Importantly, the T2WI signal characteristics of focal liver lesions are not merely descriptive: mild-to-moderate T2 hyperintensity is recognized as an ancillary feature favoring malignancy in Liver Imaging Reporting and Data System version 2018 (LI-RADS), and its presence can modify the final LI-RADS category[20, 21]. Therefore, evaluating whether the DL HASTE and BLADE sequences yield comparable T2WI signal characteristics is clinically relevant beyond subjective image quality.

Therefore, the purpose of this study was to prospectively compare the image quality and T2WI signal characteristics of the T2-weighted DL HASTE sequence with the BLADE sequence for focal liver lesions at 3 T MRI, using a larger patient population.

Material and Methods

This prospective study was approved by the Ethics Review Committee of Zhongshan Hospital, Fudan University (Approval No.: B2020-372R) and conducted in accordance with the ethical principles of the Declaration of Helsinki. All participants provided written informed consent.

Patients

Between July 2023 and March 2024, three hundred and nine consecutive adult participants undergoing liver MRI for clinical indications were prospectively enrolled. The inclusion and exclusion criteria are presented in the patient flow diagram (Fig. 1).

MR Imaging Data

Imaging was performed on a 3 T scanner (MAGNETOM Prisma; Siemens Healthineers, Erlangen, Germany). Signal reception used an 18-channel body array coil together with an integrated 32-channel spine coil. The imaging protocol comprised the following: (a) a research T2-weighted DL HASTE sequence acquired with 2 breath-holds; (b) a conventional T2-weighted BLADE sequence with navigator triggering positioned over the liver dome; (c) diffusion-weighted imaging (DWI); and (d) pre-contrast T1-weighted phase imaging followed by dynamic post-contrast T1-weighted volumetric-interpolated breath-hold examination (VIBE) acquired at the arterial (20–30 s), portal venous (60–70 s), transitional (180 s), and hepatobiliary (HBP, 20 min) phases. Gadoxetic acid (Primovist, Bayer HealthCare Pharmaceuticals Inc.) was given as an intravenous bolus at 0.025 mmol/kg. Table S1 provides further technical details for each sequence.

DL Reconstruction for HASTE

The DL HASTE images were reconstructed using a variational network [16] that had undergone training on clinical 1.5 T and 3 T MAGNETOM scanners (Siemens Healthcare). Inputs to the network consisted of precalculated coil-sensitivity maps derived from a separate reference scan, k-space data, and bias field correction. Within the unrolled network,

iterations were first carried out with trainable extrapolation steps to enforce data consistency, without additional image regularization, so that the reconstruction initially focused on parallel imaging. Subsequently, neural-network-based image regularization was incorporated to improve overall image quality[11, 14].

Qualitative MRI Analysis

Two radiologists (reader 1 and reader 2, with 10 and 8 years of abdominal MRI experience, respectively) independently reviewed the T2-weighted DL HASTE and BLADE sequences in a randomized order. The following qualitative features were assessed: overall image quality; artifacts, including in-plane respiratory motion artifact, through-plane respiratory motion artifact, and other ghosting artifacts (e.g., those arising from bowel peristalsis or vascular pulsation); sharpness of the liver margin; hepatic vessel margin; pancreatic duct margin; homogeneity of fat suppression; strength of fat suppression; conspicuity of the liver smallest lesion; and the presumed nature of that lesion. Reviewers were instructed to identify the smallest liver lesion and to grade its conspicuity from 1 to 5 (1, “unreadable”; 2, “poor”; 3, “moderate”; 4, “good”; 5, “excellent”), as well as to assign its presumed nature (difficult to determine; liquid; solid; mixed). All remaining items were scored on a 5-point scale (1–5) (Table S2).

Quantitative MRI Analysis

The two radiologists performed quantitative measurements to evaluate the relative contrast between liver parenchyma and focal liver lesions. For each sequence, the total number of focal liver lesions and the size of the smallest visible lesion were documented. To assess liver signal, a circular region of interest (ROI) measuring 20 mm in diameter was positioned within a homogeneous area of liver parenchyma that was free of vessels and artifacts. For contrast assessment, a circular ROI of maximum size was placed within the largest liver lesion (> 1 cm), covering the entire lesion. The mean signal intensity (SI) and corresponding standard deviation (SD) were recorded for each ROI.

The signal-to-noise ratio (SNR) was derived as:

$$SNR = \frac{SI_{liver}}{SD_{liver}}$$

where SI_{liver} and SD_{liver} represent the mean value and standard deviation of the liver SI, respectively.

The lesion-to-liver CNR was derived as:

$$CNR = \frac{|SI_{lesion} - SI_{liver}|}{SD_{liver}}$$

where SI_{lesion} is the mean SI of the liver lesion; SI_{liver} and SD_{liver} are the mean value and standard deviation of the SI of the adjacent healthy liver, respectively.

T2WI Signal Characteristic Analysis

For liver lesions exceeding 10 mm, the two radiologists independently performed T2WI signal characteristic analysis while blinded to the other liver MRI sequences and to clinical information. Each lesion was assigned to one of three categories based on its signal intensity on T2-weighted images: markedly hyperintense, mildly hyperintense, or iso-/hypointense. Markedly hyperintense lesions were regarded as suggestive of hemangioma or cyst; mildly hyperintense lesions were regarded as suggestive of solid lesions, including hepatocellular carcinoma (HCC); and iso- or hypointense lesions were classified as other. For each liver lesion, the imaging characteristics and location according to

the Couinaud classification were documented through joint analysis with the six other liver MRI sequences and clinical features, and this served as the reference standard. Results obtained from each T2-weighted sequence were then calculated and compared.

Complementary Analysis

A complementary analysis focused on supernumerary liver lesions that were visible exclusively on the T2-weighted DL HASTE sequence but not on the BLADE sequence, or vice versa. To establish whether a lesion was visible on these sequences, a final consensus review was conducted four weeks after the individual review sessions. A lesion was considered visible if it appeared hyperintense on diffusion-weighted imaging, or if it appeared hyperintense or hypointense on pre-contrast and/or post-contrast sequences. For each supernumerary lesion, size and location according to the Couinaud classification were recorded.

Statistical Analysis

The Kolmogorov-Smirnov test was applied to determine whether data followed a normal distribution. Acquisition times between the two sequences were compared using the Mann-Whitney U test. Differences in image quality scores and quantitative measurements between the two sequences were assessed with the paired Wilcoxon signed rank test. Agreement between the two readers was evaluated using intra-class correlation coefficients (ICC) and kappa coefficients, interpreted as follows: 0.00–0.20, no agreement; 0.21–0.40, weak agreement; 0.41–0.60, moderate agreement; 0.61–0.80, strong agreement; and 0.81–1.00, almost perfect agreement. The individual equivalence index was used to evaluate the interchangeability of T2WI signal characteristics for focal liver lesions between the two sequences, with results required to fall within the exchangeability limits of ± 5% [22, 23]. Statistical analyses were carried out using SPSS software (version 27.0) and R software (version 3.6.1). A P value < 0.05 was considered statistically significant.

Results

Participant Characteristics

A total of 309 participants were prospectively included. Of 316 eligible adult patients, we excluded 3 who refused to participate in the study and 4 with incomplete MRI dataset (Fig. 1). The mean participant age was 52.1 years ± 11.6 (SD) (age range, 19–81 years), including 217 male and 92 female participants. Table 1 shows the baseline characteristics of the participants. The most common referral reason was chronic hepatopathy follow-up (24.6%).

Table 1
Patient Characteristics and Referral Information

Characteristic	P Value
Study population	309
Age (y) *	52.1 ± 11.6
Gender	217 (70.2)
Male	92 (29.8)
Female	25.6 ± 4.7
Body mass index (kg/m^2) *	86 (27.8)
Background liver tissue	211 (72.2)
Liver cirrhosis	76 (24.6)
None	43 (13.9)
Indication for MRI	68 (22.0)
Chronic hepatopathy follow-up	59 (19.1)
HCC follow-up	63 (20.4)
Follow-up of other hepatic tumors	
Characterization of incidental hepatic findings	
Other	

Note—Unless otherwise indicated, data are number of patients, with percentage in parentheses. SD, standard deviation; MRI, Magnetic resonance imaging; HCC, hepatocellular carcinoma.

*Data are continuous variables, reported as means ± standard deviations.

Acquisition Time

The median acquisition time of the T2-weighted DL HASTE sequence was significantly shorter than that of the BLADE sequence (34 seconds [IQR, 34–34 seconds] vs 169 seconds [IQR, 158–181 seconds], respectively; P < 0.001), with a 79% reduction in acquisition time (Fig. 4).

Qualitative Analysis

The qualitative MR imaging findings are described in Table 2 and Fig. 2. T2-weighted DL HASTE sequence received significantly higher scores for artifact (P < 0.001; Fig. 2–3), pancreatic duct margin (P < 0.001; Fig. 2–3), homogeneity of fat suppression (P = 0.002), strength of fat suppression (P < 0.001), and conspicuity of the liver smallest lesion (P < 0.001) than the BLADE sequence. No statistical difference was identified in the overall image quality, sharpness of liver margin, hepatic vessel margin, and presumptive nature of the smallest lesion between the DL HASTE sequence and BLADE sequence (P > 0.05). In addition, no significant difference was observed in the T2WI signal characteristic classification between the two sequences (P = 0.391).

Table 2
Qualitative MR Imaging Findings of the T2-weighted DL HASTE and BLADE sequences

Variable	DL HASTE	BLADE	P Value
Overall image quality	5 (4, 5)	5 (4, 5)	0.257
Artifact	5 (5, 5)	5 (4, 5)	< 0.001
In-plane respiratory motion	5 (5, 5)	5 (5, 5)	< 0.001
Through-plane respiratory motion	5 (5, 5)	5 (5, 5)	< 0.001
Other ghosting artifact	5 (5, 5)	5 (5, 5)	< 0.001
Sharpness of liver margin	5 (4, 5)	5 (4, 5)	0.746
Hepatic vessel margin	5 (4, 5)	5 (4, 5)	0.303
Pancreatic duct margin	5 (5, 5)	5 (4, 5)	< 0.001
Homogeneity of fat suppression	5 (5, 5)	5 (4, 5)	0.002
Strength of fat suppression	5 (5, 5)	5 (4, 5)	< 0.001
Conspicuity of the liver smallest lesion	5 (5, 5)	5 (4, 5)	0.019
Presumptive nature of the smallest lesion*	192 (100)	181 (100)	0.157
Difficult to determine	1 (0.5)	2 (1.1)	0.391
Liquid	125 (65.1)	116 (64.1)	
Solid	60 (31.2)	58 (32.0)	
Mixed	6 (3.2)	5 (2.8)	
T2WI signal characteristic*	161 (100)	161 (100)	
Markedly hyperintense	93 (57.8)	92 (57.1)	
Mildly hyperintense	67 (41.6)	66 (41.0)	
Iso- or hypointense	1 (0.6)	3 (1.9)	

Note—Unless otherwise indicated, data are median (interquartile range). DL HASTE, half-Fourier acquisition single-shot turbo spin echo using deep learning.

*Data are number of patients, with percentage in parentheses.

Quantitative Analysis

The quantitative MR imaging findings are described in Table 3. Significantly more liver lesions were identified using the DL HASTE sequence than the BLADE sequence, especially for lesions smaller than 10mm ($P < 0.001$). We identified 776 lesions on the DL HASTE sequence versus 719 lesions on the BLADE sequence, with a total of 506 and 458 lesions smaller than 10mm, respectively. No statistical difference was identified for detected lesions larger than 10mm ($P = 0.853$) between the two sequences. No statistical difference was identified in the size of the smallest lesion ($P = 0.083$) and the SNR value of the liver parenchyma between the DL HASTE sequence and BLADE sequence ($P = 0.095$).

Table 3
Quantitative MR Imaging Findings of the T2-weighted DL HASTE and BLADE sequences

Variable	DL HASTE	BLADE	P Value
Number of lesions	1 (1, 3)	1 (1, 3)	< 0.001
total	776	719	< 0.001
Number of lesions (< 10 mm)	1 (0, 2)	1 (0, 2)	0.083
total	506	458	0.095
Size of the smallest lesion (mm)	3 (2, 8)	3 (2, 9)	< 0.001
SNR	11.64 (8.99, 15.30)	12.07 (8.84, 15.44)	< 0.001
CNR	41.02 (16.29, 66.10)	31.06 (11.99, 53.04)	0.359
All	73.49 (56.89, 101.69)	52.69 (31.09, 64.36)	0.314
Cyst	45.67 (38.76, 63.44)	43.73 (32.73, 62.90)	0.102
Hemangioma	10.37 (6.46, 12.47)	8.26 (5.64, 11.75)	0.508
FNH	17.74 (10.83, 24.90)	16.37 (7.82, 21.12)	
HCC	8.42 (1.17, 29.04)	9.06 (1.69, 28.20)	
MET			

Note—Data are median (interquartile range). DL HASTE, half-Fourier acquisition single-shot turbo spin echo using deep learning; SNR, signal- to-noise ratio; CNR, contrast-to-noise ratio; FNH, focal nodular hyperplasia; HCC, hepatocellular carcinoma; MET, metastatic tumor.

The CNR values of all liver lesions larger than 10mm were significantly better for the DL HASTE sequence (median, 41.02; IQR, 16.29–66.10) than the BLADE sequence (median, 31.06; IQR, 11.99–53.04; P < 0.001), especially for cyst (P < 0.001; Fig. 4 and Fig. S1). No statistical difference was identified in the CNR values of hemangioma, focal nodular hyperplasia (FNH), HCC, and metastatic tumor (MET) between the DL HASTE sequence and BLADE sequence (P > 0.05).

T2WI Signal Characteristics and Interchangeability

As described above, no significant systematic difference was observed in the T2WI signal characteristic classification between the two sequences (P = 0.391). The intra- and inter-protocol reader agreement and individual equivalence indexes for this classification are summarized in Table 4. A total of 161 lesions larger than 10 mm were assessed in both the DL HASTE and BLADE sequences. The three most common lesions detected were cyst (51 of 161; 31.7%), hemangioma (43 of 161; 26.7%), and HCC (48 of 161; 29.8%). All focal liver lesions were pathologically proven or had typical MRI findings based on a joint analysis with the six other liver MRI sequences.

Table 4
Intra- and Inter-protocol Reader Agreement for T2WI Signal Characteristic Classification of Focal Liver Lesions between T2-weighted DL HASTE and BLADE Sequences, and Individual Equivalence Index

Variable	Intraprotocol Assessment between DL HASTE sequence		Intraprotocol Assessment between BLADE sequence		Interprotocol Assessment between DL HASTE and BLADE sequences		Individual Equivalence Index (%) *
	No. of Examinations	Kappa value	No. of Examinations	Kappa value	No. of Examinations	Kappa value	
All	161 (100.0)	0.97	161 (100.0)	0.95	161 (100.0)	0.92	1.9 (0.38, 5.37)
Cyst	51 (31.7)	1.00	51 (31.7)	1.00	51 (31.7)	1.00	0.0 (0.00, 6.98)
Hemangioma	43 (26.7)	1.00	43 (26.7)	1.00	43 (26.7)	0.91	2.3 (0.06, 12.27)
Solid lesions	67 (41.6)	0.97	67 (41.6)	0.95	67 (41.6)	0.91	3.0 (0.36, 10.36)
FNH	9 (5.6)	1.00	9 (5.6)	1.00	9 (5.6)	1.00	0.0 (0.00, 3.63)
HCC	48 (29.8)	0.95	48 (29.8)	0.94	48 (29.8)	0.88	4.2 (0.51, 14.25)
MET	10 (6.2)	1.00	10 (6.2)	1.00	10 (6.2)	1.00	0.0 (0.00, 3.85)

Note—DL HASTE, half-Fourier acquisition single-shot turbo spin echo using deep learning; FNH, focal nodular hyperplasia; HCC, hepatocellular carcinoma; MET, metastatic tumor.

* Data in parentheses are 95% CIs.

Both intra- and inter-protocol reader agreement (DL HASTE vs. BLADE) for the T2WI signal characteristic classification of all liver lesions were strong to excellent (Kappa values ranging from 0.88 to 1.00), with benign lesions (Kappa values ranging from 0.91 to 1.00) and malignant lesions (Kappa values ranging from 0.88 to 1.00). The interreader agreement of the DL HASTE sequence and the BLADE sequence showed no difference than that of the BLADE sequence alone, with a maximum disagreement of 4.2% (95% CI: 0.51, 14.29). In summary, all absolute individual equivalence indexes were included in the limits of equivalence of 5%. Representative image results of lesions are depicted in Fig. 5–6 and Fig. S1.

Agreement Analysis

Intra-class correlation coefficients between the two readers for the DL HASTE sequence and the BLADE sequence range from strong to excellent (ICC, 0.85–0.96; ICC, 0.81–0.97; respectively) for the overall image quality, artifact, sharpness of liver margin, hepatic vessel margin, pancreatic duct margin, homogeneity of fat suppression, strength of fat suppression, conspicuity of the liver smallest lesion and presumptive nature of the smallest lesion. It was excellent for the two sequences (ICC, 0.89–0.97; ICC, 0.83–0.9; respectively) for the number of focal liver lesion detected, the size of the smallest lesion, SNR value of the liver parenchyma and the CNR value of lesion.

Complementary analysis

Of the 59 supernumerary lesions visible only on the DL HASTE sequence, 55 (93.2%) were true-positives that were also visible on the other MRI sequences, and 4 (6.8%) were false-positives (vascular cross-section). The true-positives were

mainly located on segments 2 (16 lesions; 29%) and 8 (13 lesions; 24%). All 2 supernumerary lesions visible only on the T2 BLADE-weighted sequence were true-positives.

Discussion

The study evaluated the qualitative and quantitative performance of the T2-weighted DL HASTE sequence and the BLADE sequence for 3 T liver MRI. The results suggest that the DL HASTE sequence can reduce acquisition time and artifacts while detecting more liver lesions and improving lesion CNR (especially cysts) compared to the BLADE sequence. Moreover, the two sequences showed similar performance in the T2WI signal characterization of focal liver lesions.

The results of our study are consistent with previous studies, both at 1.5 T and 3 T MRI [14, 16–19]. One possible explanation for these results is the intrinsic differences between the T2-weighted DL HASTE sequence and the BLADE sequence (i.e. single-shot TSE and multi-shot TSE). Second, the DL HASTE sequence was performed within only two breath-holds, each lasting approximately 12 seconds, which helps reduce motion artifacts and slice discontinuity, thereby improving lesion detection rates, especially for small lesions. Thirdly, the application of DL techniques has the potential to improve the image quality, reduce the total acquisition time and improve the CNR of the lesions.

The previous studies included small numbers of participants and were limited in scope to evaluating perceived image quality rather than T2WI signal characterization of focal liver lesions[17, 18]. Our study showed that the two sequences had comparable performance in T2WI signal characterization for benign and malignant liver lesions. The point estimates of the individual equivalence index were within the pre-specified 5% limit for all lesions, supporting the interchangeability of the DL HASTE sequence with the BLADE sequence for 3 T liver MRI at the overall level, although subgroup estimates were limited by small sample sizes.

In our study, the CNR values of liver cysts larger than 10mm were significantly better for the DL HASTE sequence than the BLADE sequence. No statistical difference was identified in the CNR values of hemangioma, FNH, HCC, and MET between the DL HASTE sequence and BLADE sequence. We speculate that the strong T2 weighting of the DL HASTE sequence may improve the detection of cystic lesions, but does not decrease the detection of solid lesions, especially in the detection of mild-moderate T2WI hyperintensity of malignant tumors in the Liver Imaging Reporting and Data System (LI-RADS).

Of the 55 true-positives of supernumerary lesions visible only on the DL HASTE sequence, the majority may be explained by motion artifacts or slice discontinuity on the T2-weighted BLADE sequence. These lesions were mainly localized in liver segments #2 and #8, which are affected by more artifacts, especially those related to cardiac motion, making it difficult to detect these lesions. Of the four false-positives on the DL HASTE sequence, three appeared to be caused by signal cancellation defects in the liver vessels. Therefore, these focal intravascular hypersignal could lead to false-positive detections, especially if they are only present on a single slice. This artifact is identifiable in large and medium vessels because it follows the vessel path, and analysis of the overlying and underlying slices allows the vessel to be traced, confirming that the artifact is intravascular.

T2-weighted MRI is important for the detection and characterization of liver lesions, including in the LI-RADS algorithm and recommended in the liver MRI protocol [20, 24], even in the era of hepatobiliary contrast agents. Half-Fourier acquisition patterns allow a reduction in acquisition time at the expense of an increase in TE, resulting in reduced sensitivity for tumor detection and the diagnostic accuracy. The use of DL reconstruction allows higher acceleration in HASTE acquisition, thus allowed the use of TE values close to those of BLADE sequences, resulting in similar sensitivity for tumor detection and the diagnostic accuracy.

DL techniques have been widely used in artificial intelligence research and practice in recent years. Moreover, DL techniques are increasingly being used in image acquisition, particularly in MR image reconstruction (including liver,

shoulder, spine, knee, prostate, etc.), with the aim of improving image quality by identifying and mitigating artifacts in accelerated acquisition[25–31]. We speculate that DL techniques will have greater potential waiting to be developed in the field of MR image reconstruction.

The study has several limitations. Firstly, this was a single-center study, and the subgroup analyses for FNH and MET were based on a limited number of lesions. Secondly, the supernumerary liver lesions visible only on the T2-weighted DL HASTE sequence or the BLADE sequence were identified by joint analysis with other MRI sequences rather than by histopathological confirmation. Thirdly, previous studies used single breath-hold DL HASTE. However, in our current study with a feet-first position for abdominal exams, the stricter SAR limits often caused single breath-hold DL HASTE to exceed these limits. As a result, we opted for two breath-holds. Further optimization of the SAR calculation model for feet-first positioning or refinement of RF pulses to reduce energy is needed. Finally, these results may not be generalized to all available MR systems as the DL reconstruction mode used in this study is proprietary.

In conclusion, the T2-weighted DL HASTE sequence led to shorter examination time, higher capability for small lesion, higher image quality and with comparable T2WI signal characteristic for focal liver lesions compared with the BLADE sequence.

Abbreviations

CNR Contrast
to-noise ratio

Declarations

Conflict of Interest:

Two authors of this manuscript declare relationships with the following companies: Cai-Xia Fu and Dominik Nickel are employees of Siemens Healthineers. These two authors were not involved in the acquisition or analysis of the data and did not have access to patient data. These two authors participated in the development of the DL HASTE sequence that was provided to us as part of a research project. The other authors of this manuscript declare no relationships with any companies, whose products or services may be related to the subject matter of the article.

Ethics approval and consent to participate

This prospective study was approved by the Ethics Review Committee of Zhongshan Hospital, Fudan University (Approval No. : B2020-372R) and conducted in accordance with the ethical principles of the Declaration of Helsinki. All participants provided written informed consent.

Consent for publication

All authors have read the final version of this manuscript, agree with its content, and consent to its submission for publication. All authors take full responsibility for the work presented herein.

Funding:

This study has received funding by National Natural Science Foundation of China [Grant NO: 82272078; 82672637] and Clinical Research of Shanghai Municipal Health Commission [Grant NO: 20254Y0008].

Author Contribution

Authors contributions: S.Y.D., Y.D., M.S.Z., and S.X.R. contributed to the conceptualization and study design. S.Y.D., J.H.W., D.Z.G., W.T.W., X.S.C., D.L.L. W.S. and C.Z.C. contributed to data collection and resource provision, including MRI imaging and clinical data. S.Y.D, J.H.W., D.Z.G., W.T.W., and Y.D. conducted data curation and statistical analysis. S.Y.D drafted the original manuscript. W.T.W., C.X.F., D.N., Y. Ding and S.X.R. provided critical review, manuscript editing, and supervision.

Data Availability

Data Availability: The datasets generated and/or analysed during the current study are not publicly available due Data security, but are available from the corresponding author on reasonable request.

References

1. Girardet R, et al. The combination of non-contrast abbreviated MRI and alpha foetoprotein has high performance for hepatocellular carcinoma screening. Eur Radiol. 2023;33(10):6929–38.
2. Starmans MPA, et al. Automated Assessment of T2-Weighted MRI to Differentiate Malignant and Benign Primary Solid Liver Lesions in Noncirrhotic Livers Using Radiomics. Acad Radiol. 2024;31(3):870–9.
3. Jia L, et al. Deep learning-based MRI model for predicting P53-mutated hepatocellular carcinoma. BMC Med Imaging. 2025;25(1):506.
4. Chen J et al. The Use of Non-Contrast Abbreviated MRI for the Detection of Recurrent Hepatocellular Carcinoma in Postoperativ Surveillance. J Magn Reson Imaging, 2026.
5. Nanko S, et al. Usefulness of the application of the BLADE technique to reduce motion artifacts on navigation-triggered prospective acquisition correction (PACE) T2-weighted MRI (T2WI) of the liver. J Magn Reson Imaging. 2009;30(2):321–6.
6. Canellas R, et al. Abbreviated MRI Protocols for the Abdomen. Radiographics. 2019;39(3):744–58.
7. Donato H, Liver MRI, et al. From basic protocol to advanced techniques. Eur J Radiol. 2017;93:30–9.
8. Lee MG, et al. Fast T2-weighted liver MR imaging: comparison among breath-hold turbo-spin-echo, HASTE, and inversion recovery (IR) HASTE sequences. Abdom Imaging. 2000;25(1):93–9.
9. Schlemper J, et al. A Deep Cascade of Convolutional Neural Networks for Dynamic MR Image Reconstruction. IEEE Trans Med Imaging. 2018;37(2):491–503.
10. Hammernik K, et al. Learning a variational network for reconstruction of accelerated MRI data. Magn Reson Med. 2018;79(6):3055–71.
11. Herrmann J, et al. Development and Evaluation of Deep Learning-Accelerated Single-Breath-Hold Abdominal HASTE at 3 T Using Variable Refocusing Flip Angles. Invest Radiol. 2021;56(10):645–52.
12. Herrmann J, et al. Diagnostic Confidence and Feasibility of a Deep Learning Accelerated HASTE Sequence of the Abdomen in a Single Breath-Hold. Invest Radiol. 2021;56(5):313–9.
13. Tan Q, et al. Optimized deep learning-accelerated single-breath-hold abdominal HASTE with and without fat saturation improves and accelerates abdominal imaging at 3 Tesla. BMC Med Imaging. 2025;25(1):369.
14. Mulé S, et al. Fast T2-weighted liver MRI: Image quality and solid focal lesions conspicuity using a deep learning accelerated single breath-hold HASTE fat-suppressed sequence. Diagn Interv Imaging. 2022;103(10):479–85.
15. Han S, et al. Evaluation of HASTE T2 weighted image with reduced echo time for detecting focal liver lesions in patients at risk of developing hepatocellular carcinoma. Eur J Radiol. 2022;157:110588.

16. Shanbhogue K, et al. Accelerated single-shot T2-weighted fat-suppressed (FS) MRI of the liver with deep learning-based image reconstruction: qualitative and quantitative comparison of image quality with conventional T2-weighted FS sequence. Eur Radiol. 2021;31(11):8447–57.
17. Ichinohe F, et al. Usefulness of Breath-Hold Fat-Suppressed T2-Weighted Images With Deep Learning-Based Reconstruction of the Liver: Comparison to Conventional Free-Breathing Turbo Spin Echo. Invest Radiol. 2023;58(6):373–9.
18. Wary P, et al. Deep learning HASTE sequence compared with T2-weighted BLADE sequence for liver MRI at 3 Tesla: a qualitative and quantitative prospective study. Eur Radiol. 2023;33(10):6817–27.
19. Ginocchio LA, et al. Accelerated T2-weighted MRI of the liver at 3 T using a single-shot technique with deep learning-based image reconstruction: impact on the image quality and lesion detection. Abdom Radiol (NY). 2023;48(1):282–90.
20. (AASLD). A.A.f.t.S.o.L.D., LI-RADS® CT/MRI v2018 Core. 2018.
21. Chen J, et al. LI-RADS category 3, 4, and M observations: a multiple parameters diagnostic model for hepatocellular carcinoma. Acta Radiol. 2023;64(12):2977–86.
22. Othman AE, et al. Free-breathing Arterial Spin Labeling MRI for the Detection of Pulmonary Embolism. Radiology. 2023;307(3):e221998.
23. Obuchowski NA, Subhas N, Schoenhagen P. Testing for interchangeability of imaging tests. Acad Radiol. 2014;21(11):1483–9.
24. Chernyak V, et al. Version 2018: Imaging of Hepatocellular Carcinoma in At-Risk Patients. Radiology. 2018;289(3):816–30. Liver Imaging Reporting and Data System (LI-RADS).
25. Xie Y, et al. Prospective Comparison of Standard and Deep Learning-reconstructed Turbo Spin-Echo MRI of the Shoulder. Radiology. 2024;310(1):e231405.
26. Almansour H, et al. Deep Learning Reconstruction for Accelerated Spine MRI: Prospective Analysis of Interchangeability. Radiology. 2023;306(3):e212922.
27. Herrmann J, et al. Deep Learning MRI Reconstruction for Accelerating Turbo Spin Echo Hand and Wrist Imaging: A Comparison of Image Quality, Visualization of Anatomy, and Detection of Common Pathologies with Standard Imaging. Acad Radiol. 2023;30(11):2606–15.
28. Bischoff LM, et al. Deep Learning Super-Resolution Reconstruction for Fast and Motion-Robust T2-weighted Prostate MRI. Radiology. 2023;308(3):e230427.
29. Li Q, et al. Deep learning-accelerated T2WI: image quality, efficiency, and staging performance against BLADE T2WI for gastric cancer. Abdom Radiol (NY). 2024;49(8):2574–84.
30. Song YS, et al. Clinical efficacy of motion-insensitive imaging technique with deep learning reconstruction to improve image quality in cervical spine MR imaging. Br J Radiol. 2024;97(1156):812–9.
31. Yan L, et al. Ultrafast T2-weighted MR imaging of the urinary bladder using deep learning-accelerated HASTE at 3 Tesla. BMC Med Imaging. 2025;25(1):284.

Figures

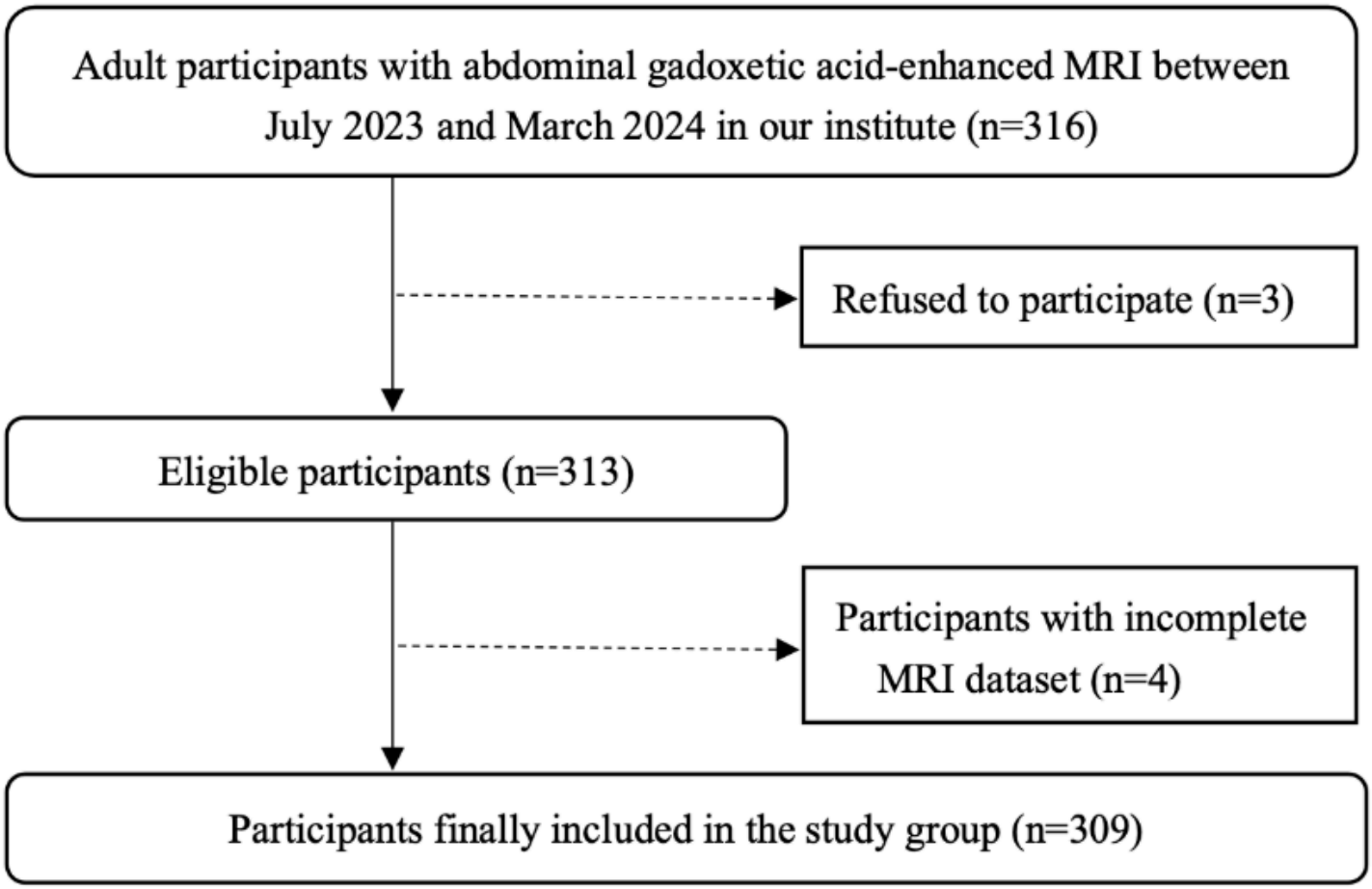


Figure 1

The flow diagram shows the inclusion and exclusion criteria for the study.

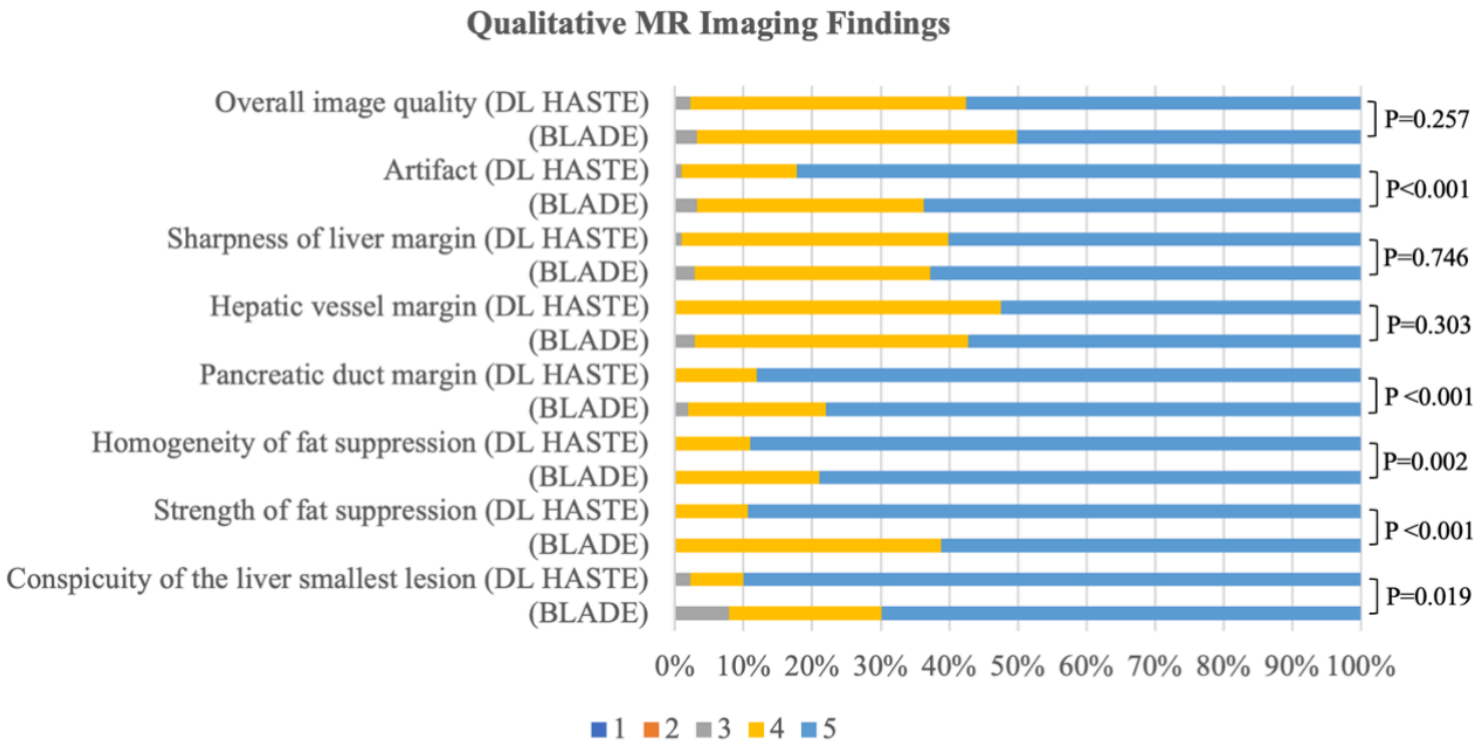


Figure 2

Bar charts showing a summary of the qualitative five-grade scoring of the T2-weighted DL HASTE and BLADE sequences. DL HASTE, half-Fourier acquisition single-shot turbo spin echo using deep learning.

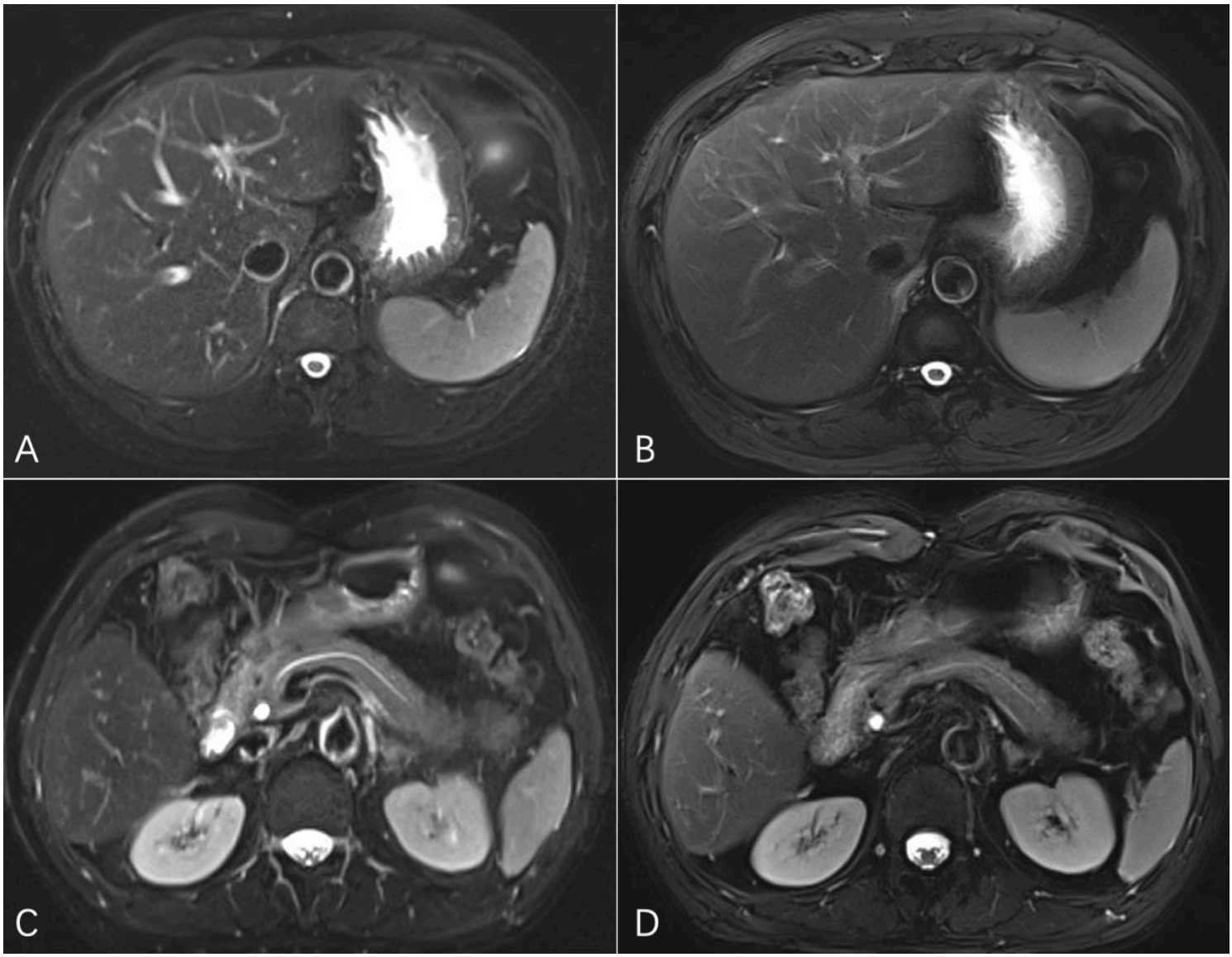


Figure 3

The T2-weighted DL HASTE axial image (A) shows fewer motion artifacts than the BLADE axial image (B); the DL HASTE axial image (C) shows better pancreatic duct margin than the T2-weighted BLADE axial image (D). DL HASTE, half-Fourier acquisition single-shot turbo spin echo using deep learning; CNR, contrast-to-noise ratio.

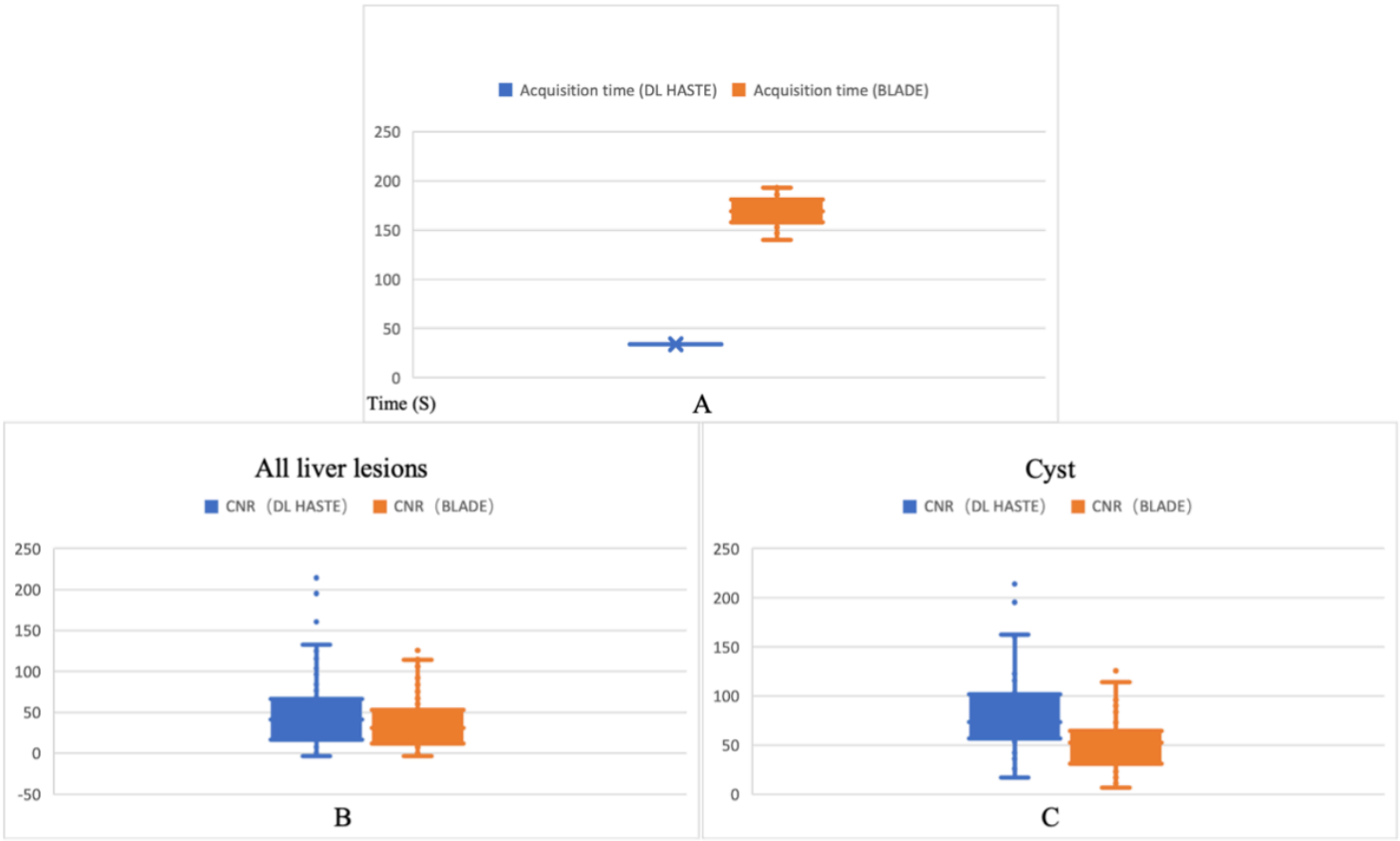


Figure 4

(A) Differences in acquisition time between the T2-weighted DL HASTE and BLADE sequences (P <0.001); (B) differences in the CNR values of all liver lesions larger than 10mm between the two sequences (P <0.001); (C) differences in the CNR values of cyst larger than 10mm between the two sequences (P <0.001). DL HASTE, half-Fourier acquisition single-shot turbo spin echo using deep learning; CNR, contrast-to-noise ratio.

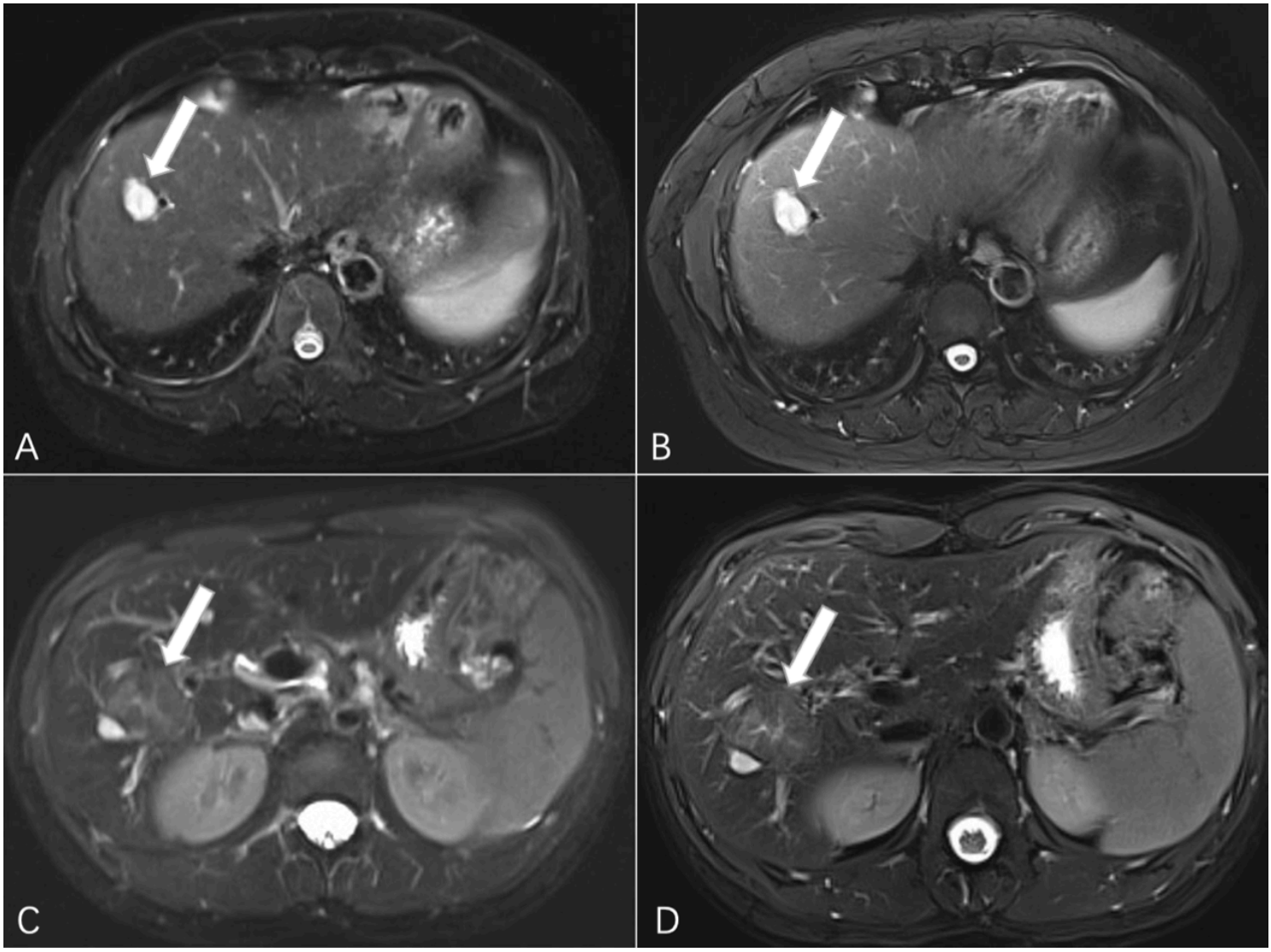


Figure 5

Characterization of benign liver lesions. The T2-weighted DL HASTE axial image (A) shows similar conspicuity for hemangioma than the BLADE axial image (B); CNR of the lesion in DL HASTE sequence and BLADE sequence are 47.63 and 43.73, respectively. The DL HASTE axial image (C) shows similar conspicuity for focal nodular hyperplasia than the BLADE axial image (D); CNR of the lesion in DL HASTE sequence and BLADE sequence are 12.91 and 8.95, respectively. Both readers classified the hemangioma as markedly hyperintense and the focal nodular hyperplasia as mildly hyperintense on both sequences. DL HASTE, half-Fourier acquisition single-shot turbo spin echo using deep learning; CNR, contrast-to-noise ratio; T2WI, T2-weighted imaging.

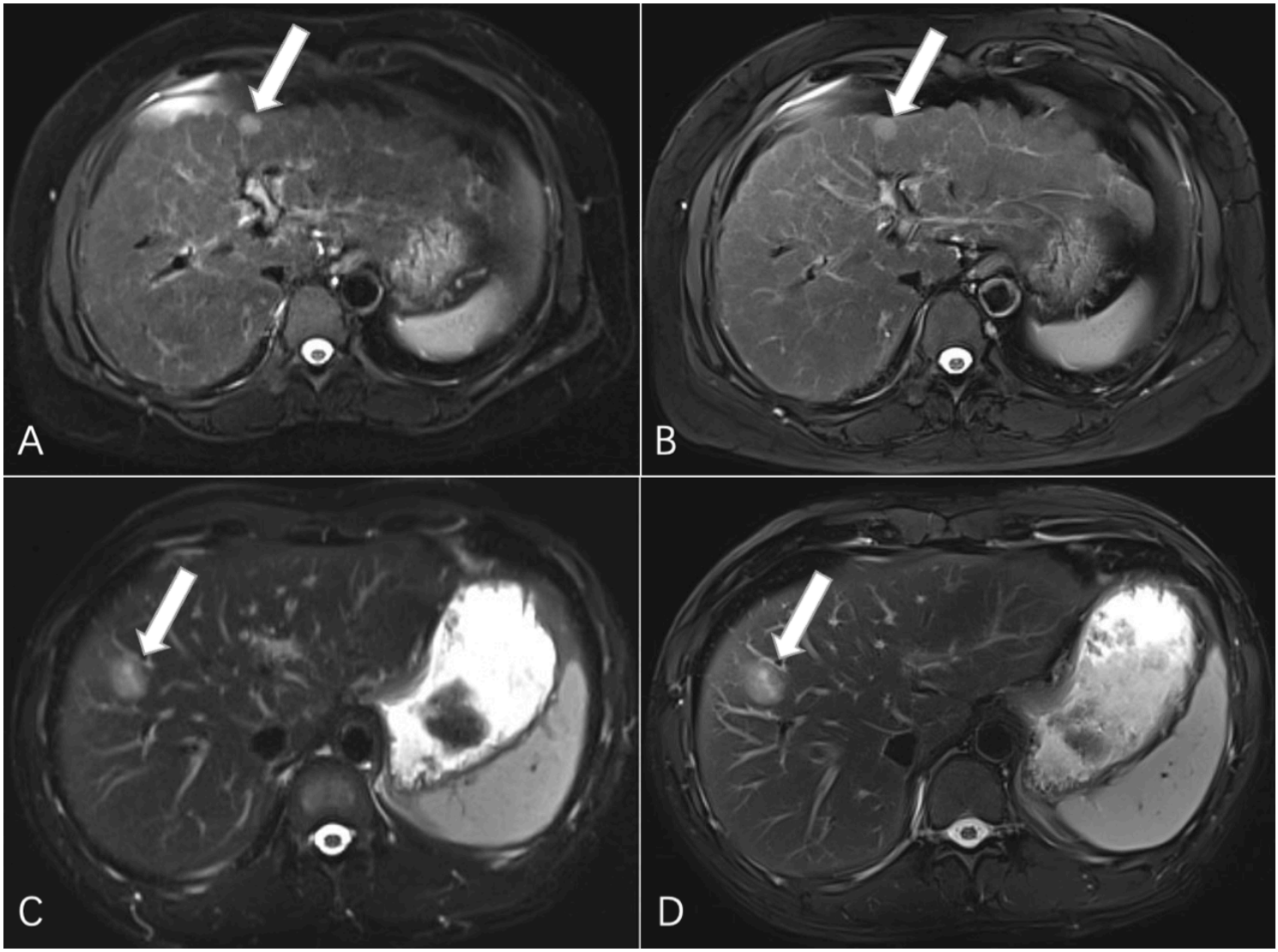


Figure 6

Characterization of malignant liver lesions. The T2-weighted DL HASTE axial image (A) shows similar conspicuity for hepatocellular carcinoma than the BLADE axial image (B); CNR of the lesion in DL HASTE sequence and BLADE sequence are 24.34 and 19.18, respectively. The DL HASTE axial image (C) shows similar conspicuity for metastatic tumorthan the BLADE axial image (D); CNR of the lesion in DL HASTE sequence and BLADE sequence are24.25 and 28.18, respectively. Both readers classified the two lesions as mildly hyperintense on both sequences. DL HASTE, half-Fourier acquisition single-shot turbo spin echo using deep learning; CNR, contrast-to-noise ratio; T2WI, T2-weighted imaging.

Supplementary Files

This is a list of supplementary files associated with this preprint. Click to download.

- SupplementalFileforReview.docx